Molecular Suppression of the Pimerization of Viologens (= 4,4′-Bipyridinium Derivatives) Attached to Nanocrystalline Titanium Dioxide Thin-Film Electrodes

by **Michael Felderhoff**, **Susanne Heinen**, **Ngongo Molisho**, **Simona Webersinn**, and **Lorenz Walder***

Institut für Chemie, Universität Osnabrück, Barbarastr. 7, D-49069 Osnabrück

Dedicated to Prof. Dr. *Frank Seela* on the occasion of his 60th birthday

Twelve viologens, *i.e.*, 4,4′-bipyridinium derivatives **1**–**12**, were examined for their use as electrochromic material when attached to nanocrystalline titanium dioxide thin-film electrodes. Eight of these (**1**–**4**, **7**–**8**, **10**, and **12**) are new, and their synthesis is included. The modifier compounds consist of one to four bipyridinium subunits with linear or dendritic architecture, equipped with one to three TiO_2-anchoring phosphonate groups. They are tailored for high electrochromic dynamics (large absorbance change upon reduction) and low extent of pimerization (= charge-transfer (CT) complexation of viologen cation radicals). A new graphical method is presented for the discrimination of simple dilution phenomena and more complex structural effects on the extent of pimerization in the surface-attached viologen layer.

1. Introduction. – 1,1′-Dialkyl, 1,1′-dibenzyl, or 1,1′-diphenyl-4,4′-bipyridinium salts (viologens) have been known for several decades for their intense coloration (ε *ca.* 10000–30000) when reduced to the cation radical, rendering them interesting as cathodic electrochromic material [1]. There have been doubts in the past with respect to their use in practical devices because of the long-term stability of organic electrochromophores in general and viologens in particular. However, the most successful commercial application of an electrochromic device at present is based on viologens. *Gentex Corp.* (Zeeland, MI, USA) has introduced a self-dimming rear-view electrochromic mirror for the automotive sector, which uses a viologen dissolved in a thin solution that is sandwiched between two optically transparent electrodes (OTE) [2].

Several attempts to improve the switching time between the colored and bleached state have been described in the literature. The principal idea is to use electrode-surface-confined viologens and thus prevent slow diffusional processes of the electrochromophore. A single molecular monolayer of viologens on an ideally smooth OTE yields only minor changes in absorbance upon reduction (*Eqn. 1*). In *Eqn. 1*, ΔA is the electrochemically switchable absorbance change (for many applications desirable close to 1), $\Gamma_{e.c.}$ the surface concentration of electrochromic centers (e.c.) on a smooth electrode [mol cm^{-2}] (typically $2.8 \cdot 10^{-10}$ mol cm^{-2} for a head-on-anchored viologen with two large counter ions), and ε the extinction coefficient of the colored state ($1 \cdot 10^4$ or higher for a viologen) assuming negligible absorption for the bleached state; the factor $1 \cdot 10^3$ is the correction for the cm^2-dm^3 transition. Thus, in order to achieve a ΔA value of 1, 357 ($1/2.8 \cdot 10^{-3}$) molecular monolayers of the electrochromophore are required in the above example. This can be realized either using a film of poly-viologen corresponding to 357 monolayers on a smooth electrode, or a viologen monolayer

attached to a three-dimensional electrode with a surface-roughness factor (R) of 357 (*Eqn. 2*).

$$\Delta A_{\text{monolayer, smooth}} = \Gamma_{\text{e.c.}} \cdot \varepsilon \cdot 10^3 \approx 2.8 \cdot 10^{-10} \cdot 10^4 \cdot 10^3 = 2.8 \cdot 10^{-3} \quad (1)$$

$$\Delta A_{\text{multilayer,rough}} = \Gamma_{\text{e.c.}} \cdot \varepsilon \cdot 10^3 \cdot R \quad (2)$$

Nanocrystalline thin-film titanium dioxide electrodes have a mesoporous structure with a surface-roughness factor (R) of *ca.* 100 per μm film thickness. This semiconductor material is optically transparent in the visible range, exhibits good electronic conductivity if polarized in the negative range of the flat band potential, and shows high affinity towards molecular surface modifiers equipped with anchoring groups (a.g.) such as phosphonates. Beside its well-known use for sensitized photovoltaics [3], it finds increasing interest as an electrode material for electrochromics [4]. The principal electrochromic phenomenon of viologen adsorbed on thin-film TiO_2 electrodes (in the following abbreviated as: vio-on-TiO_2) has been demonstrated earlier and is depicted in *Fig. 1* [5]. More recently, prototype electrochromic filters, displays, and mirrors have been described [6][7], and considerable effort has been made in view of TiO_2-attachable bipyridinium salts exhibiting green [6] and pink [8] electrochromism. Another parameter we tried to optimize is enhanced absorptivity [6], which can be principally achieved by the use of thicker TiO_2 layers, *i.e.*, a larger R value in *Eqn. 2*. However, TiO_2 always contains a certain amount of light-scattering centers so that the overall optical quality with respect to haze drops linearly with the film thickness. Another approach towards increased dynamics (ΔA) consists in anchoring head-on-di- or trimeric viologens (molecular amplification, h) in *Fig. 1*). We expected at first that the electrochromic centers (e.c.) per surface area ($\Gamma_{\text{e.c.}}$) could be doubled or tripled in this way. However, steric hindrance related to the restricted space within the mesopores (*e* in *Fig. 1*) reduces the surface concentration leading to a maximum enhancement factor of *ca.* 2 for oligomeric viologens [6]. Moreover, for high surface concentrations, we observed a blue shift of the main absorbance in the VIS spectrum coupled with a delayed oxidation. This was interpreted as a charge-transfer (CT)-type dimerization of the radical cations, also known as pimerization [9–11]. Pimerization processes are characterized by an interaction between the π-systems of the two radicals, causing a blue shift (increased absorbance at 537 nm, a broad absorption in the 800 to 1100 nm region, and a concomitant decrease at 605 nm). From studies of viologens in solution, it is known that the pimer equilibrium (see *Eqn. 3*) depends strongly on the solvent [12–14], temperature, concentration [15], and structure [16–18]. Thus, the same viologen studied spectroelectrochemically in solution may show no indication of pimerization, but may exhibit extensive pimerization if packed in a monolayer on the TiO_2 walls because of the high two-dimensional concentration. As mentioned earlier, we found for the pimerized state a sluggish electrochemical oxidation as compared to the free radical cation. For the further development of vio-on-TiO_2-based electrochromic devices, it is therefore crucial to find ways to prevent – or at least to reduce the extent of – pimerization, while keeping the surface concentration as high as possible. Methods known to suppress pimerization in solution include, for example, the addition of cyclodextrin, but this is not expected to be successful in the present surface-confined case [19][20].

$$2\ \text{Vio}^{+\bullet} \rightleftarrows (\text{Vio}^{+\bullet})_2 \quad (3)$$

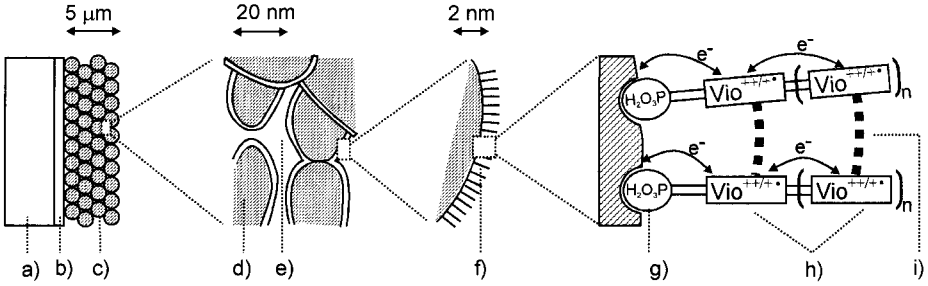

Fig. 1. *Nanocrystalline and molecular amplification of the electrochromic response of viologens attached to a nanocrystalline titanium dioxide thin-film electrode.* a) Glass support; b) optically transparent electrode (OTE); c)–f) nanocrystalline amplification; c) thin-film nanocrystalline titanium dioxide layer; d) nanocrystal; e) mesopore; f) electrochromic monolayer; g)–i) molecular amplification and pimerization; g) phosphonate anchoring group (a.g.); h) (oligo-)viologen with one or several electrochromic centers (e.c.) and anchoring groups (a.g.); i) pimerization of two neighboring radical cations.

We report here the synthesis of eight new mono- and oligomeric viologens equipped with phosphonate TiO_2-anchoring groups, followed by a comparative spectroelectrochemical study of 12 viologens (including four earlier-described compounds) attached to nanocrystalline TiO_2 thin film electrodes (*Scheme 1*) [6]. The main purpose was to find those structural properties and coordination characteristics that allow optimization high surface concentration of electroactive centers ($\Gamma_{e.c.}$) at a low degree of pimerization of the surface-bound viologen in its cation-radical state.

2. Results and Discussion. – 2.1. *Synthesis.* All compounds **1**–**12** were obtained from the corresponding diethyl phosphonates **1a**–**12a** as bromide salts by hydrolysis in 1M HBr (*Scheme 1*). The synthesis of **5**, **6**, **9**, and **11** has been described earlier [6]. The monomeric compounds **1a**–**3a** were obtained from the reaction of 4,4′-bipyridine with diethylphosphonomethyl triflate (=(diethoxyphosphinyl)methyl trifluoromethanesulfonate) [21] followed by counter-ion exchange with tetrabutylammonium bromide (Bu_4NBr), with diethyl 2-bromoethylphosphonate, and with diethyl 3-bromopropylphosphonate [22], respectively. The dimeric viologen **4a** was prepared from 1,1″-[1,4-phenylenebis(methylene)]bis[4,4′-bipyridinium] bis(hexafluorophosphate) [6] and diethyl 2-bromoethylphosphonate, followed by ion exchange with Bu_4NBr. Compounds **7a** and **8a** were prepared by monoalkylation of 2-methyl-4,4′-bipyridine [23] and 2,2′-dimethyl-4,4′-bipyridine [24] with diethyl 2-bromoethylphosphonate, followed by a second alkylation step with bromoethane and iodoethane, respectively.

The synthesis of compounds **10** and **12** is shown in *Scheme 2.* Starting from the known precursor **13** [6], the key intermediate **15** was prepared by reaction with 4,4′-bipyridine, followed by treatment with ammonium hexafluorophosphate (NH_4PF_6). The also required bipyridinium salt **14** was prepared by consecutive alkylation of 4,4′-bipyridine with bromoethane and α,α'-dibromo-*p*-xylene (=1,4-bis(bromomethyl)-benzene), again followed by ion exchange with NH_4PF_6. Compound **15** was then alkylated with bromide **14** to yield ester **10a** after treatment with Bu_4NBr. The bis[bipyridinium] salt **15** was also used for the preparation of intermediate **16** by alkylation with 1,3,5-tris(bromomethyl)benzene [25] followed by ion exchange with NH_4PF_6. Reaction of **16** with 2 equiv. of 1-ethyl-4,4′-bipyridinium hexafluorophos-

Scheme 1. *Electrochromic Compounds* **1**–**12** *for* TiO_2*-Electrode Modification*

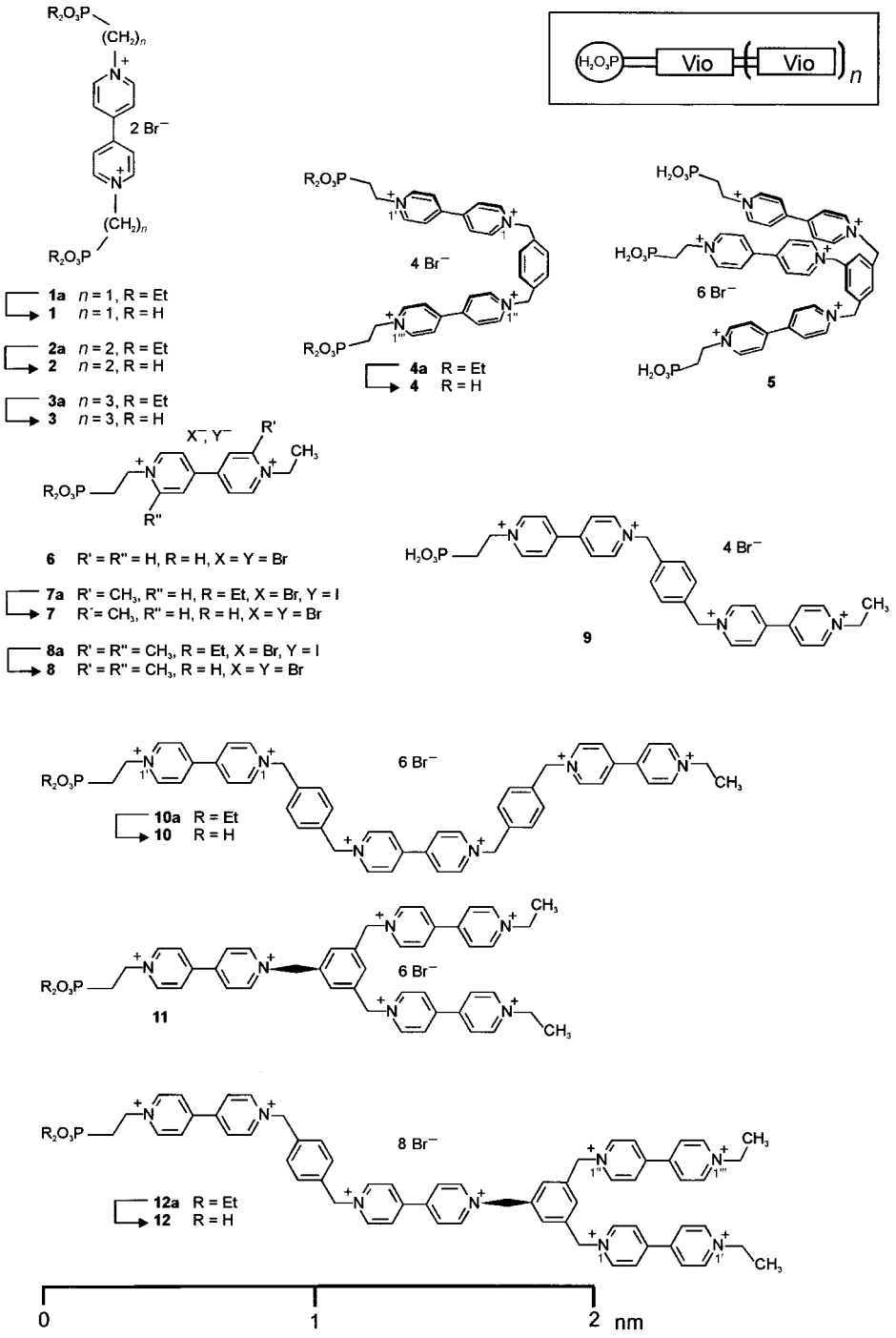

Scheme 2. *Synthesis of Compounds* **10** *and* **12**

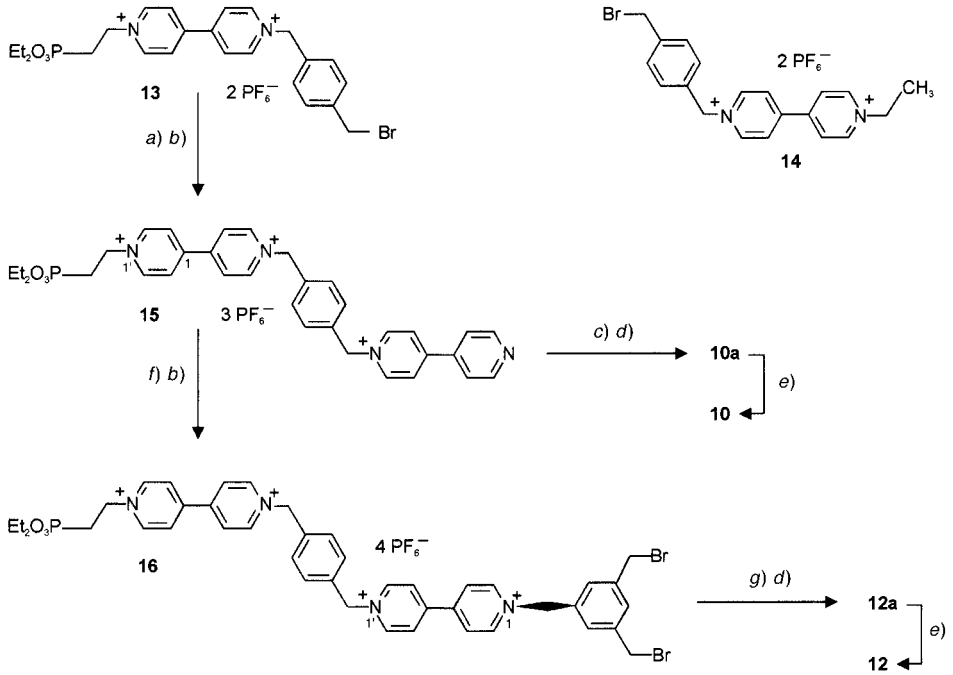

a) 4,4′-Bipyridine, MeCN. *b*) Aq. NH_4PF_6. *c*) **14**, MeCN. *d*) TBABr, MeCN. *e*) 1M HBr. *f*) 1,3,5-Tris-(bromomethyl)benzene, MeCN. *g*) *N*-Ethyl-4,4′-bipyridinium hexafluorophosphate, MeCN.

phate [26] yielded the tetrameric viologen **12a** after treatment with Bu_4NBr. The purity of all compounds was checked by ^{1}H-NMR (for details, *cf. Exper. Part*).

2.2. *Spectroelectrochemical Results.* Two- to five-μm thick TiO_2 electrodes were coated with monolayers of compound **1**–**12** from a EtOH/H_2O solution as described earlier or from a DMSO solution [6]. The resulting vio-on-TiO_2 electrodes were checked for their surface concentration in electrochromic centers ($\Gamma_{e.c.}$, *Eqn. 2*) and for the extent of viologen pimerization ($=(\Gamma_{e.c.,pim}/\Gamma_{e.c.})\cdot 100$, *cf. Exper. Part*, *Eqns. 4*–*7*) by spectroelectrochemistry and coulometry. Notably, $\Gamma_{e.c.}$ is a normality, *i.e.*, the number of the electrochromic centers (e.c. = viologen subunits) per molecule times the surface concentration of the compound. Spectroelectrochemistry yielded generally more reliable results as compared to coulometry (from integration of slow-scan cyclic voltammograms) because the faradayic current was difficult to separate from TiO_2-charging currents, especially for compounds with more negative $E_{1/2}$. The pimerization, $\Gamma_{e.c.}$, and $E_{1/2}$ data (see *Table*) revealed substantial differences in surface concentration and in the degree of pimerization for the different compounds coated under identical conditions, *e.g.*, **6**- or **2**-on-TiO_2 show a similar surface concentration but a definitely different pimerization (*Fig. 2*)

To study the influence of the viologen surface concentration ($\Gamma_{e.c.}$) on the pimerization, the diluent octylphosphonic acid ($C_8H_{17}PO_3H_2$) was co-adsorbed with **6** at solution concentration ratios [**6**]/[$C_8H_{17}PO_3H_2$] from 50 to 0.25 [27]. The resulting

Table. *Pimerization and Surface Concentration of Compounds* **1**–**12** *Reduced to the Radical-Cationic State in Monolayers on Nanocrystalline Titanium Dioxide Thin-Film Electrodes*

	e.c.[a])	a.g.[b])	e.c./a.g.	$\Gamma_{e.c.} \cdot 10^{-8}$ [mol cm^{-2}][c])	Pimerization [%][d])	$E_{1/2}$ [V] *vs.* Ag/AgCl
1	1	2	0.5	2.4 (1)	12	– 0.61 (– 0.25)[e])
2	1	2	0.5	9.3 (5.5)	18	– 0.49 (– 0.33)[e])
3	1	2	0.5	7.4 (6)	17	– 0.50 (– 0.31)[e])
4	2	2	1	18 (14)	39	– 0.44
5	3	3	1	21 (17)	33	– 0.46
6	1	1	1	10	54	– 0.42
7	1	1	1	8.9	52	– 0.45
8	1	1	1	8.3	27	– 0.62
9	2	1	2	19	52	– 0.39
10	3	1	3	15	42	– 0.40
11	3	1	3	14	44	– 0.42
12	4	1	4	14	43	– 0.38

[a]) Equiv. electrochromic centers (e.c.). [b]) Equiv. anchoring groups (a.g.). [c]) Average values from spectroelectrochemistry (coulometry values in brackets if different), normalized for 5-μm TiO_2-film thickness. The values for **4** and **5** depend on the TiO_2 sample; reproducibility is ±10%. [d]) Determined from VIS spectroscopy at 537 and 605 nm according to *Eqns. 4–7*; the experimental error is ±10%. [e]) Values in brackets: from CV of the corresponding esters in homogeneous solution (DMF 0.1M Bu_4NClO_4).

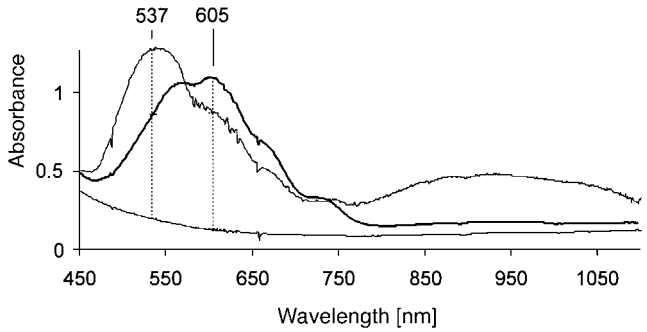

Fig. 2. *VIS Spectra of* **6**-*on-TiO*$_2$ (thin line) *and* **2**-*on-TiO*$_2$ (thick line) *after electrochemical reduction under controlled potential conditions and common baseline for the oxidized states.* **6**-on-TiO_2 exhibits *ca.* 55% pimerization and $\Gamma_{e.c.} = 1 \cdot 10^{-7}$ mol cm^{-2}, whereas **2**-on-TiO_2 exhibits *ca.* 20% pimerization at a similar surface concentration, as calculated from the absorbance differences (dotted lines) and from *Eqns. 4–7.* Approximately 5-μm thick TiO_2 layers were used and potentiostated at *ca.* 120 mV in the negative range of $E_{1/2}$; solvent: MeCN/0.3M $LiClO_4$.

TiO_2 electrodes exhibited reduced $\Gamma_{e.c.}$ ranging from 98 to 23% of the value observed for undiluted **6**-on-TiO_2. The pimerized portion follows this trend as a monotonic function, *i.e.*, pure **6**-on-TiO_2 shows 54% pimerization, but (**6** diluted to 23%)-on-TiO_2 exhibits only 20% (*Fig. 3*, *Exper. Part*). Similar results were observed when salicylic acid (=2-hydroxybenzoic acid) was used instead of octylphosphonic acid. Principally, the results are in agreement with the general trend observed for pimerization as a function of concentration (or intramolecular distances) for monomeric viologens in solution [19], for polymeric viologens [20], viologen cyclophanes [11], and viologen dendrimers [28]. It is not clear if, in our case, co-adsorption leads to a statistical or ordered arrangement of the two competing compounds, or if large islands consisting of pure viologen and octylphosphonate areas are formed (see also below).

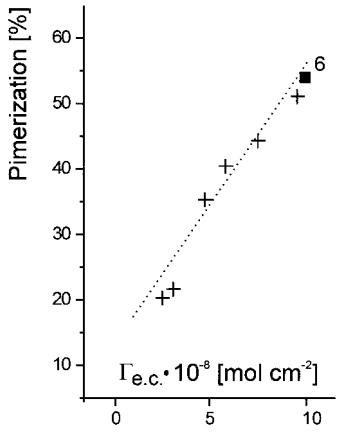

Fig. 3. *Radical-cation pimerization as a function of surface concentration for* **6***-on-TiO*$_2$ (■) *and* **6***(diluted)-on-TiO*$_2$ (+). Co-adsorbing diluent was octylphosphonic acid.

The same type of plot (*Fig. 4*) for all the compounds **1**- to **12**-on-TiO_2 in their undiluted state scatters, but the occupied segment reflects again the general trend, *i.e.*, the higher the surface concentration, the higher the pimerization. The monotonic function resulting from the dilution experiment of **6**-on-TiO_2 (*Fig. 3*) is also reported in *Fig. 4*. In the following, we try to interpret the offset of some compounds from this curve on the basis of their structural differences and specific coordination properties as compared to the standard **6**.

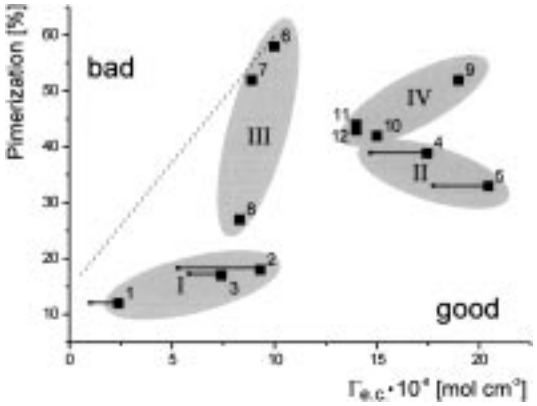

Fig. 4. *Radical-cation pimerization as a function of surface concentration of the electrochromic centers for compounds* **1**- to **12***-on-TiO*$_2$ (without dilution). Clusters observed are: double-anchored monomeric (I), multiple-anchored oligomeric (II), single-anchored monomeric (III), and single-anchored oligomeric viologens. Dotted line: results from *Fig. 3*; horizontal error bars are given (values from the *Table*). The terms 'good' and 'bad' refer to the electrochromic-device application.

According to their structural similarities, **1**–**12** can be gathered in four clusters (gray regions I–IV in *Fig. 4*). Cluster I contains compounds with one electrochromic center (e.c.) and two anchoring groups (a.g.) (e.c./a.g. = 0.5). Assuming double

anchoring, these compounds lie flat on the TiO_2 and occupy a larger surface area compared to the standard **6** with e.c./a.c. = 1, *i.e.*, they are, therefore, expected to show a lower surface concentration, as observed experimentally for **1** but not for **2** and **3**. From the same model, one would expect increasing pimerization with the number of methylene groups between the phosphonate moiety and the bipyridinium N-atom, because the required coplanar stacking of two neighboring viologens becomes possible when the viologen plane rotates into a conformation perpendicular to the TiO_2 surface (*Fig. 5*). The same rotation may explain the differences in surface concentration of **1**–**3** discussed above. Cyclic voltammetry shows a significant jump in $E_{1/2}$ from **3**- or **2**-on-TiO_2 to **1**-on-TiO_2, whereas the corresponding esters **1a**–**3a** measured in homogeneous solution show the opposite trend in $E_{1/2}$ (*cf. Table*). This phenomenon may again be related to the unique orientation of **1**. The surface concentration for compounds **1**- to **3**-on-TiO_2 as measured by cyclic voltammetry is inaccurate because of interfering capacitive currents in the negative potential range.

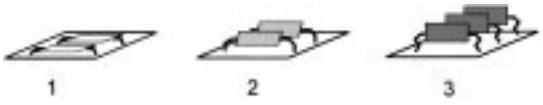

Fig. 5. *Model of the surface attachment of compounds* **1**- *to* **3**-*on-*TiO_2. The length of the linker between phosphonate and bipyridinium increases stepwise (1, 2, and 3 CH_2 groups, respectively). This reduces the strain of a co-planar arrangement perpendicular to the surface and leads to intensified pimerization in the series.

Cluster II (see *Fig. 4*) contains the oligomeric viologens **4** and **5** with two and three electrochromic centers and as many anchoring groups (e.c./a.g. = 1). Assuming double and triple anchoring, respectively, they are expected to occupy a similar surface area per electrochromic center as **6**. Actually, we observed in some cases the same $\Gamma_{e.c.}$ for **4**, **5**, and **6** if the ±10% error is taken into account, but on other TiO_2 samples, much higher surface concentrations were observed, indicating difficulties controlling single or double (or triple) coordination. Significant is the reduced pimerization for **4** and **5** compared to the standard **6**. One explanation is the unique combination of double or triple anchoring and the 'xylylic' or 'mesitylic' bridging. This holds the electrochromic centers in place and suppresses the required conformational changes for pimer formation in the reduced state.

Cluster III represents the monomeric viologens **6**–**8**, all of which have identical *N*-substituents and e.c./a.g. = 1, but which have increasing steric hindrance in a monolayer because of the methyl substituents at the aromatic moiety. Typically, the $E_{1/2}$ drops in line with the number of electron-donating Me substituents. The pimerization drops much faster than expected from the dilution line of **6**, which may indicate island formation in case of the dilution experiment (*Fig. 3*) and a more efficient 'dilution' in case of built-in steric hindrance.

In cluster IV, the oligomeric viologens **9**–**12** with a single anchoring group and e.c./a.g. = 2, 3, 3, and 4, respectively, are assembled. As reported earlier for a similar set of compounds, the expected increase in $\Gamma_{e.c.}$ up to a factor of four is not observed. Compound **9** with two viologen subunits shows double $\Gamma_{e.c.}$, but **10**–**12** are all in the intermediate range between standard **6** and dimer **9**. Obviously, an increasing part of the pore walls becomes inaccessible for the larger electrochromic compounds **10**–**12**

(*cf. Scheme 1* for approximate lengths). The reasons may be narrow channels between pores that do not allow the passage or steric hindrance of **10**–**12** when coated on opposite pore walls. As with compounds **4** and **5**, we found a strong dependence also of $\Gamma_{e.c.}$ on the TiO_2 structure (porosity, pore diameter).

To the best of our knowledge, pimerization *vs.* surface-concentration plots as presented in *Fig. 4* are new. They allow qualitative discrimination between clusters of structurally related compounds. The axes surface concentration and pimerization correspond to 'good' and 'bad' with respect to the electrochromic device. It is, therefore, possible, as in the case of combinatorial chemistry, to derive a structural guess for planning the next synthesis. The future will show whether *Fig. 4*, with its limited set of compounds, can give us a reliable structural guess.

The authors thank *Pilkington Germany GmbH* for financial support and the *Institute of Applied Photovoltaics* (*INAP*), Gelsenkirchen, Germany, for the supply of TiO_2-coated OTE.

Experimental Part

General. Solvents/electrolytes: MeCN/$LiClO_4$ (both *Fluka, puriss.*) were used as purchased. EtOH (*p.a.*) was from *Merck*. ^{1}H-NMR: *Bruker Avance 250* (250 MHz); chemical shifts δ in ppm, coupling constant J in Hz.

TiO_2-Electrodes. The colloidal TiO_2 soln. and TiO_2-coated OTEs (2- to 5-μm thick) were prepared for low haze by the *Institute of Applied Photovoltaics* (*INAP*), Gelsenkirchen, Germany, or prepared according to a literature process [29]. Viologen-coating: the TiO_2 electrodes were modified with compounds **1**–**12** by coating from a EtOH/H_2O 7:3 soln. of viologen ($c = 0.5-3\cdot10^{-3}$ M) for 12 h [6]. The dilution experiment was done from EtOH/H_2O using 6 different mixtures of **6** and octylphosphonic acid [27] with [**6**] + [$C_8H_{19}PO_3$] = $5\cdot10^{-4}$ M.

Spectro- and Electrochemical Equipment and Methods. A *PAR-173* potentiostat (*Princeton Applied Research*) in combination with a *HP8453* diode-array spectrometer (*Hewlett Packard*) was used for the spectroelectrochemical measurements. An *Autolab PGSTAT 20* (from *ECO Chemie*, Utrecht, Netherlands) was used for cyclic voltammetry. A 1-cm quartz cuvette was fitted to the bottom of a *Metrohm* cell. The OTEs were cut usually to *ca*. 1-cm^2 pieces that fit into the cuvette. The reference electrode was Ag/AgCl in sat. KCl soln. separated by a salt bridge from the cell, the counter electrode was usually a Pt-wire. The spectroelectrochemical measurements of vio-on-TiO_2 were performed under potentiostatic conditions at *ca*. 120 mV in the negative range of $E_{1/2}$, spectra were recorded when the absorption was constant, *i.e.*, after a few seconds. The most pronounced wave (usually the cathodic $vio^{++}/vio^{+\cdot}$ wave) in the cyclic voltammogram ($\nu = 5$ to 20 mV/s) was used to integrate the charge and to calculate the coulometric surface concentration. All electrochemical measurements were conducted in MeCN/0.3M $LiClO_4$. The degree of pimerization [%] and the total-surface concentration ($\Gamma_{e.c.}$) was determined from the observed absorbances at 605 and 537 nm (A_{605} and A_{537}, resp.) by *Eqns. 4–7*, with $\Gamma_{e.c.,\ mon}$ and $\Gamma_{e.c.,\ pim}$ corresponding to the surface concentrations [mol cm^{-2}] of the electrochromic centers in monomeric and pimerized form, resp. Identical extinction coefficients from the literature were used for all compounds **1**–**12** in their pure monomeric (mon) or pimerized (pim) form: $\varepsilon_{mon,605} = 13000$, $\varepsilon_{mon,537} = 6500$, $\varepsilon_{pim,537} = 14500$, and $\varepsilon_{pim,605} = 1175$ assuming that all the viologens **1**–**12** exhibit extinction coefficients similar to dibenzylviologen [11].

$$\Gamma_{e.c.,\ mon} = (A_{605}\cdot\varepsilon_{pim,537} - A_{537}\cdot\varepsilon_{pim,605})/(1000\ (\varepsilon_{mon,605}\cdot\varepsilon_{pim,537} - \varepsilon_{mon,537}\cdot\varepsilon_{pim,605})) \quad (4)$$

$$\Gamma_{e.c.,pim} = (A_{537}\cdot\varepsilon_{mon,605} - A_{605}\cdot\varepsilon_{mon,537})/(1000\ (\varepsilon_{mon,605}\cdot\varepsilon_{pim,537} - \varepsilon_{mon,537}\cdot\varepsilon_{pim,605})) \quad (5)$$

$$\Gamma_{e.c.} = \Gamma_{e.c.,mon} + \Gamma_{e.c.,pim} \quad (6)$$

$$\text{pimerization } [\%] = (\Gamma_{e.c.,\ pim}/\Gamma_{e.c.})\cdot 100 \quad (7)$$

The preparation and characterization of compounds **5**, **6**, **9**, and **11** were described recently [6].

1,1′-Bis(phosphonomethyl)-4,4′-bipyridinium Dibromide (**1**). At 0°, 4,4′-bipyridine (200 mg, 1.28 mmol) and (diethoxyphosphinyl)methyl trifluoromethanesulfonate [21] (3.65 g, 12.2 mmol) were dissolved in MeCN (6 ml), heated to r.t., and stirred for 3 days. The product was precipitated with Et_2O and dissolved in MeCN.

Dropwise addition of a sat. Bu_4NBr soln. in MeCN and drying of the precipitate *in vacuo* gave **1a** (415 mg, 51%). A portion of **1a** (300 mg, 0.49 mmol) was dissolved in 1M HBr (40 ml) and refluxed for 96 h. The solvent was evaporated and the residue dried *in vacuo:* **1** (241 mg, 98%). ^{1}H-NMR (D_2O): 8.80 (*d*, *J* = 5.7, 4 H); 8.33 (*d*, *J* = 6.8, 4 H); 4.70 (*d*, *J* = 13.2, 4 H).

1,1′-Bis(2-phosphonoethyl)-4,4′-bipyridinium Dibromide (**2**). A soln. of 4,4′-bipyridine (1 g, 6.4 mmol) and diethyl 2-bromoethylphosphonate (18 ml, 101 mmol) in MeCN (6 ml) was stirred at 65° for 5 days. The product **2a** precipitated, was washed with Et_2O, and dried *in vacuo* (2.5 g, 60%). As described for **1**, **2a** was transformed to **2** (99%). ^{1}H-NMR (D_2O): 8.94 (*d*, *J* = 6.7, 4 H); 8.33 (*d*, *J* = 6.6, 4 H); 4.72 (*dt*, *J* = 10.8, 5.4, 4 H); 2.29 (*dt*, *J* = 17.9, 7.7, 4 H).

1,1′-Bis(3-phosphonopropyl)-4,4′-bipyridinium Dibromide (**3**). A soln. of 4,4′-bipyridine (80 mg, 0.51 mmol) and diethyl 3-bromopropylphosphonate [22] (400 mg, 1.54 mmol) in MeCN (1 ml) was stirred at 65° for 10 days, and **3a** was isolated as described for **2a** (205 mg, 60%). Hydrolysis of **3a** as described for **1** yielded **3** (98 mg, 82%). ^{1}H-NMR (D_2O): 9.38 (*d*, *J* = 5.1, 4 H); 8.79 (*d*, *J* = 5.1, 4 H); 4.77 (*m*, 4 H); 2.17 (*m*, 4 H); 1.60 (*m*, 4 H).

1,1″-[1,4-Phenylenebis(methylene)]bis[1′-(2-phosphonoethyl)-4,4′-bipyridinium] Tetrabromide (**4**). A mixture of 1,1″-[1,4-phenylenebis(methylene)]bis[4,4′-bipyridinium] bis(hexafluorophosphate) [6] (1 g, 1.42 mmol) and diethyl 2-bromoethylphosphonate (4 g, 16.32 mmol) in MeCN (25 ml) was stirred at 85° for 96 h. After cooling, the mixture was added to a soln. of Bu_4NBr (923 mg) in MeCN (10 ml) and kept for 12 h at 0°. The precipitate was filtered off, washed with MeCN and CH_2Cl_2, and dried *in vacuo:* **4a** (1.075 g, 71%) as a yellow solid. A portion of **4a** (500 mg, 0.47 mmol) was hydrolyzed as described for **1**: **4** (307 mg, 69%). Yellow solid. ^{1}H-NMR (D_2O): 8.99 (*d*, *J* = 6.8, 8 H); 8.49 (*d*, *J* = 5.6, 4 H); 8.37 (*d*, *J* = 6.4, 4 H); 7.46 (*s*, 4 H); 5.82 (*s*, 4 H); 4.76 (*dt*, *J* = 12.8, 4 H); 2.31 (*dt*, *J* = 17.9, 4 H).

1-Ethyl-2-methyl-1′-(2-phosphonoethyl)-4,4′-bipyridinium Dibromide (**7**). A mixture of 2-methyl-4,4′-bipyridine [23] (128 mg, 0.75 mmol) and diethyl 2-bromoethylphosphonate (180 mg, 0.73 mmol) were reacted at 60° for 39 h. The monoalkylated product precipitated, was divided in two portions, washed with Et_2O, and dried *in vacuo* (158 mg, 51%). The resulting 1-[2-(diethoxyphosphinyl)ethyl)-2′-methyl-4,4′-bipyridinium bromide (70 mg, 0.17 mmol) and bromoethane (0.36 g, 3.35 mmol) were heated in DMF/MeCN 1:1 (2 ml) at 65° for 9 days. The precipitated product was filtered off, washed with Et_2O, and dried *in vacuo:* **7a** (87 mg, 99%). As described for **1**, **7a** (127 mg, 0.24 mmol) was hydrolyzed: **7** (108 mg, 95%). ^{1}H-NMR (D_2O): 9.47 (*d*, *J* = 6.9, 2 H); 9.35 (*d*, *J* = 6.7, 1 H); 8.89 (*d*, *J* = 2.0, 1 H); 8.84 (*d*, *J* = 6.8, 2 H); 8.67 (*dd*, *J* = 6.6, 2.0, 1 H); 4.79–4.65 (*m*, 4 H); 3.01 (*s*, 3 H); 1.64–1.51 (*m*, 5 H).

1-Ethyl-2,2′-dimethyl-1′-(2-phosphonoethyl)-4,4′-bipyridinium Dibromide (**8**). As described for **7**, starting with 2,2′-dimethyl-4,4′-bipyridine [24] (186 mg, 1 mmol). Stepwise alkylation with diethyl 2-bromoethylphosphonate (4.9 g, 20 mmol; 96 h, 50°) and iodoethane (4.33 mmol; 72 h, 80°; 5 ml of MeCN) gave **8a** (60 mg, 44%). Hydrolysis of **8a** (60 mg, 0.102 mmol) with 1M HBr gave **8**. Hygroscopic oil. ^{1}H-NMR (D_2O): 8.76 (*d*, *J* = 6.7, 1 H); 8.72 (*d*, *J* = 6.6, 1 H); 8.14–8.12 (*m*, 2 H); 8.04 (*d*, *J* = 6.7, 2 H); 4.68 (*m*, 2 H); 4.42 (*q*, *J* = 7.3, 2 H); 2.75 (*s*, 3 H); 2.71 (*s*, 3 H); 2.17 (*dt*, *J* = 18.5, 7.9, 2 H); 1.36 (*t*, *J* = 7.3, 3 H).

1-{[4-[([4,4′-Bipyridin-1-ium]-1-yl)methyl]phenyl}methyl]-1′-[2-(diethoxyphosphinyl)ethyl]-4,4′-bipyridinium Tris(hexafluorophosphate) (**15**). A soln. of 1-{[4-(bromomethyl)phenyl]methyl}-1′-[2-(diethoxyphosphinyl)-ethyl]-4,4′-bipyridinium bis(hexafluorophosphate) (**13**) [6] (2.5 g, 3.14 mmol) and 4,4′-bipyridine (730 mg, 4.69 mmol) in MeCN (20 ml) was stirred at 60° for 7 h. A soln. of Bu_4NBr (2.06 g, 6.39 mmol) in MeCN (15 ml) was added to the cold mixture and the residue filtered off, washed with MeCN (20 ml) and dried: tribromide **15**·(3 Br^- instead of 3 PF_6^-; 2.04 g, 79%). ^{1}H-NMR (D_2O): 9.01 (*d*, *J* = 4.3, 4 H); 8.87 (*d*, *J* = 6.5, 2 H); 8.61 (*d*, *J* = 5.5, 2 H); 8.43 (*d*, *J* = 6.4, 2 H); 8.39 (*d*, *J* = 6.4, 2 H); 8.26 (*d*, *J* = 6.5, 2 H); 7.80 (*d*, *J* = 5.9, 2 H); 7.45 (*s*, 4 H); 5.82 (*s*, 2 H); 5.76 (*s*, 2 H); 4.86 (*dt*, *J* = 16.5, 7.2, 2 H); 3.96 (*q*, *J* = 7.3, 4 H); 2.64 (*dt*, *J* = 18.5, 7.2, 2 H); 1.08 (*t*, *J* = 7.1, 6 H).

Tribromide **15** (3 Br^- instead of 3 PF_6^-; 2.0 g, 2.43 mmol) was dissolved in H_2O (90 ml), and a soln. of NH_4PF_6 in H_2O (*c* = 0.613 M) was added dropwise. The precipitate was stirred for 10 min, filtered off, washed with H_2O (3 × 10 ml), and dried *in vacuo:* tris(hexafluorophosphate) **15** (2.20 g, 90%). White powder.

1-{[4-(Bromomethyl)phenyl]methyl}-1′-ethyl-4,4′-bipyridinium Bis(hexafluorophosphate) (**14**). To a soln. of 1-ethyl-4,4′-bipyridinium bromide [26] (1.70 g, 6.4 mmol) in MeCN (30 ml), 1,4-bis(bromomethyl)benzene (2.53 g, 9.6 mmol) in MeCN (10 ml) was added and heated under reflux for 6.5 h. After cooling, the precipitate was filtered off, washed with MeCN (10 ml), Et_2O (10 ml), and CH_2Cl_2 (10 ml) and dried *in vacuo:* dibromide **14** (2 Br^- instead of 2 PF_6^-; 3.23 g, 95%). ^{1}H-NMR (D_2O): 9.14 (*d*, *J* = 6.7, 2 H); 9.11 (*d*, *J* = 6.4, 2 H); 8.54–8.52 (*m*, 4 H); 7.53 (*d*, *J* = 8.0, 2 H); 7.48 (*d*, *J* = 8.0, 2 H); 5.93 (*s*, 2 H); 4.75 (*q*, *J* = 7.3, 2 H); 4.65 (*s*, 2 H); 1.69 (*t*, *J* = 7.3, 3 H).

Dibromide **14** (2 Br^- instead of 2 PF_6^-; 2.90 g, 5.48 mmol) was ion-exchanged with NH_4PF_6 as described for **15**: bis(hexafluorophosphate) **14** (3.0 g, 83%).

1-{[4-{[1′-{[4-[(1′-Ethyl-[4,4′-bipyridinium]-1-yl)methyl]phenyl}methyl][4,4′-bipyridinium]-1-yl}methyl]phenyl}methyl]-1′-(2-phosphonoethyl)-4,4′-bipyridinium Hexabromide (**10**). To a soln. of **15** (1.0 g, 0.984 mmol) in MeCN (10 ml), **14** (653 mg, 0.991 mmol) in MeCN (25 ml) was added and heated under reflux for 24 h. After cooling, Bu_4NBr (1.90 g, 5.90 mmol) was added, the mixture stirred for 15 min and then cooled to 0° for 1 h, and the solid filtered off, washed with MeCN (3 × 10 ml), and dried *in vacuo:* **10a** (315 mg, 23%). Hydrolysis of **10a** (182 mg, 0.135 mmol) as described for **1** gave **10** (166 mg, 95%). ^{1}H-NMR (D_2O): 9.01–8.90 (*m*, 12 H); 8.39–8.37 (*m*, 12 H); 7.47 (*s*, 8 H); 5.82 (*s*, 8 H); 4.79 (*dt*, 2 H); 4.51 (*m*, 2 H); 2.32 (*dt*, *J* = 17.7, 7.3, 2 H); 1.53 (*t*, *J* = 7.3, 3 H).

1-{[3,5-Bis(bromomethyl)phenyl]methyl}-1′-{[4-{[1′-[2-(diethoxyphosphinyl)ethyl][4,4′-bipyridinium]-1-yl}methyl]phenyl}methyl]-4,4′-bipyridinium Tetrakis(hexafluorophosphate) (**16**). A soln. of **15** (1.0 g, 0.984 mmol) in MeCN (10 ml) was added to 1,3,5-tris(bromomethyl)benzene [25] (1.05 g, 2.95 mmol) in MeCN (10 ml) and heated under reflux for 24 h. After cooling, Bu_4NBr (960 mg, 2.98 mmol) in MeCN (10 ml) was added. The mixture was stirred for 15 min and then cooled to 0° for 1 h, the solid filtered off, washed with MeCN (3 × 10 ml), and dried *in vacuo:* tetrabromide **16** (4 Br^- instead of 4 PF_6^-; 809 mg, 70%). ^{1}H-NMR (D_2O): 9.01–8.92 (*m*, 8 H); 8.42–8.34 (*m*, 8 H); 7.44 (*s*, 4 H); 7.36 (*s*, 1 H); 7.25 (*s*, 2 H); 5.80 (*s*, 4 H); 4.85 (*dt*, *J* = 16.4, 2 H); 4.47 (*s*, 4 H); 3.94 (*quint.*, *J* = 7.2, 4 H); 2.63 (*dt*, *J* = 18.7, 2 H); 1.05 (*t*, *J* = 7.1, 6 H).

Tetrabromide **16** (4 Br^- instead of 4 PF_6^-; 650 mg) was treated with NH_4PF_6 as described above: 710 mg (89%) of tetrakis(hexafluorophosphate) **16**.

1,1″-{5-{[1′-{[4-{[1′-(2-Phosphonoethyl)-[4,4′-bipyridinium]-1-yl]methyl}phenyl}methyl][4,4′-bipyridinium]-1-yl}methyl]-1,3-phenylenebis(methylene)}bis[1′-ethyl-4,4′-bipyridinium] Octabromide (**12**). A soln. of 1-ethyl-4,4′-bipyridinium hexafluorophosphate [26] (231 mg, 0.70 mmol) in MeCN (10 ml) was added to **16** (450 mg, 0.313 mmol) in MeCN (10 ml) and heated under reflux for 120 h. The solid was washed with MeCN and discarded. To the combined liquid phases, a soln. of Bu_4NBr (506 mg, 1.57 mmol) in MeCN (10 ml) was added, and the yellow product which precipitated was washed with MeCN (2 × 10 ml) and CH_2Cl_2 (2 × 10 ml), and dried *in vacuo:* **12a** (301 mg, 56%). As described for **1**, **12a** (200 mg, 0.117 mmol) was hydrolyzed: **12** (170 mg, 87%). Oily product. ^{1}H-NMR (D_2O): 9.03–8.94 (*m*, 16 H); 8.42–8.39 (*m*, 16 H); 7.66 (*s*, 3 H); 7.47 (*s*, 4 H); 5.86 (*s*, 6 H); 5.82 (*s*, 4 H); 4.85 (*dt*, 2 H); 4.49 (*q*, 4 H); 2.38 (*dt*, 2 H); 1.52 (*t*, *J* = 7.3 Hz, 6 H).

REFERENCES

[1] P. M. S. Monk, R. J. Mortimer, D. R. Rosseinsky, 'Electrochromism', VCH, Weinheim, 1995.
[2] H. J. Byker, to *Gentex Corp.* (Zeeland, MI), U.S. Pat. 4,902,108, 1990.
[3] B. O'Reagan, M. Grätzel, *Nature (London)* **1991**, *353*, 737.
[4] T. Gerfin, L. Walder, M. Grätzel, *Prog. Inorg. Chem.* **1997**, *44*, 345.
[5] A. Hagfeldt, L. Walder, M. Grätzel, *Proc. SPIE-Int. Soc. Opt. Eng. XIV* **1995**, *2531*, 60.
[6] F. Campus, P. Bonhôte, M. Grätzel, S. Heinen, L. Walder, *Sol. Energy Mater. Sol. Cells* **1999**, *56*, 281.
[7] R. Cinnsealach, G. Boschloo, S. N. Rao, D. Fitzmaurice, *Sol. Energy Mater. Sol. Cells* **1998**, *55*, 215; R. Cinnsealach, G. Boschloo, S. N. Rao, D. Fitzmaurice, *ibid.* **1999**, *57*, 107.
[8] R. Boehlen, M. Felderhoff, R. Michalek, L. Walder, *Chem. Lett.* **1998**, 815.
[9] E. M. Kosower, J. L. Cotter, *J. Am. Chem. Soc.* **1964**, *86*, 5524.
[10] P. M. S. Monk, R. D. Fairweather, M. D. Ingram, J. A. Duffy, *J. Chem. Soc., Perkin Trans 2* **1992**, 2039.
[11] W. Geuder, S. Hünig, A. Suchy, *Tetrahedron* **1986**, *42*, 1665.
[12] M. Itoh, E. M. Kosower, *J. Am. Chem. Soc.* **1986**, *90*, 1843.
[13] E. M. Kosower, A. Teuerstein, *J. Am. Chem. Soc.* **1976**, *98*, 1586.
[14] C. L. Bird, A. T. Kuhn, *Chem. Soc. Rev.* **1981**, *10*, 49.
[15] E. Weitz, *Ber. Dtsch. Chem. Ges.* **1942**, *79*, 1927.
[16] A. G. Evans, J. C. Evans, M. W. Baker, *J. Chem. Soc., Perkin Trans. 2* **1977**, 1787.
[17] A. G. Evans, N. K. Dodson, N. H. Rees, *J. Chem. Soc., Perkin Trans. 2* **1976**, 859.
[18] A. G. Evans, J. C. Evans, N. H. Rees, *J. Chem. Soc., Perkin Trans. 2* **1975**, 1831.
[19] A. Yasuda, H. Mori, J. Mizuguchi, *Jpn. J. Appl. Phys.* **1987**, *26*, 1352.
[20] Y. Nambu, K. Yamamoto, T. Endo, *J. Chem. Soc., Chem. Commun.* **1986**, 574.
[21] D. P. Phillion, S. S. Andrew, *Tetrahedron Lett.* **1986**, *27*, 1477.
[22] G. M. Kosolapoff, *J. Am. Chem. Soc.* **1944**, *66*, 1511.

[23] F. Minisci, F. Bertini, R. Galli, *Ger. Offen.* **1972**, *153* (3), 234.
[24] P. Leighton, J. K. M. Sanders, *J. Chem. Soc., Perkin Trans. 1* **1987**, 2385.
[25] F. Vögtle, M. Zuber, R. G. Lichtenthaler, *Chem. Ber*. **1973**, *106*, 717.
[26] J. Bruinink, C. G. A. Kregting, J. J. Ponjeé, *J. Electrochem. Soc*. **1977**, *124*, 1854.
[27] G. M. Kosolapoff, *J. Am. Chem. Soc*. **1945**, *67*, 1180.
[28] S. Heinen, L. Walder, *Angew. Chem*. **1999**, submitted.
[29] B. O'Reagan, J. Moser, M. Anderson, M. Grätzel, *J. Phys. Chem*. **1990**, *94*, 8720.

Received September 3, 1999